Original Research Article

Design and construction of a system for measuring carbon monoxide, hydrogen and methane concentrations in a co-current downdraft biomass gasifier

Abstract

Gasification is the process of producing combustible gases from solid materials such as coal, biomass or solid waste. The laboratory of Space Physics and Energy has two experimental gasifiers producing synthetic gases whose natures and concentrations must be determined. To do this, lower-cost sensors were purchased and used for determining the concentration of carbon monoxide with maximum concentration of 1.000 and 2.000 ppm. Hydrogen and methane concentration was not offered by these two commercial gas analyzers. In this paper Metal-Oxide gas sensors were used to extend the measurement range of carbon monoxide up to 4.000ppm. Hydrogen and methane concentrations up to 10.000ppm in synthetic gas produced by a wood fired co-current downdraft gasifier measurements were also enabled. These sensors have a chemical sensing element based on a layer of tin dioxide (SnO_2); whose resistivity is sensitive to nature of the gas between two sensing electrodes. This property gives these sensors a resistive electrical model whose measurand is the concentration of the input gas. This study shows that resistor R of the sensor is related to the gas concentration with an equation of the form: $\log(R/R_0) = A \log(x) + B$. With A= -0.3072, B = 0.921 for methane, A= -0.6527, B=1.3055 for carbon dioxide and A= -1.522, B = 4.5686 for hydrogen.

Keywords: Gasification, Modelling, Concentration, Carbon monoxide, Hydrogen, Methane

1. Introduction

Burkina Faso, efforts to reduce energy dependence (of populations and industries on fossil resources and wood) are being carried out through the development of renewable energy sources such as photovoltaic and thermal solar [1], [2]. To make our contribution to this concern, the Laboratory has therefore embarked on the construction of experimental gasifiers producing synthetic gases usable for the production of electricity. From May to august 2022, a first downdraft gasifier was designed and successfully tested two wood fired downdraft biomass in Burkina Faso [3], [4]. A second gasifier was designed and built from September to December 2022 in order to overcome design flaw that was found in the first gasifier during the testing's. The two gasifiers built are of the co-current type which are already used in industry from 100kW and above for their suitability, as well as their relative ease of manufacturing in developing countries.

Biomass gasification produce a synthesis gas mainly consisting of combustibles gases such as carbon monoxide, hydrogen and small amount of methane and incombustibles gases like nitrogen of the

air, car bone dioxide and water vapor [5], [6], [7], [8], [9].

The two gasifiers used commercial flue gas analyzers for measuring the produced gases concentrations. But only carbon monoxide with a maximum concentration of 1000 and 2000 ppm where was available. None of the available gas analyzers offered hydrogen and methane concentration measurement.

As said by Yulin Kong et al. [10]: "S_nO_2 has been extensively used in the detection of various gases. As a gas sensing material, S_nO_2 has excellent physical-chemical properties, high reliability, and short adsorption-desorption time". It was also found in the literature that other authors were already using cheap gas monitoring sensors for industrial applications [11], [12], [13]. It was also found that a microcontroller can be used to acquire data from numerous sensors, compute several mathematical functions and display these values [14], [15], [16]. This is why it was anticipated that the combination of these gas sensors with a microcontroller constitute a cost-effective solution for monitoring gas concentrations in our biomass gasifiers and decided to build an experimental prototype system for measuring these gases, in particular carbon monoxide, hydrogen and methane.

2. Materials and methods

2.1 Experimental setup

The gasifier used in this work is composed of several functional units:

- The reactor
- The cyclone
- The condenser
- The filter

Figure 1 bellow shows the overview of these different parts. MQ gas sensors are located on a sampling box that draw small amount of synthetic gas cleaned of tar and water vapor by the cyclone separator, the condenser and the filter.

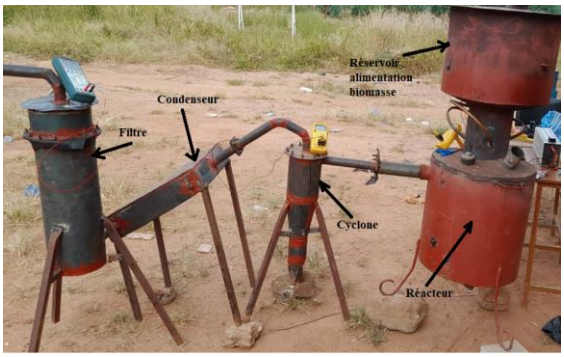

Figure 1 : Experimental setup

2.2 Methods

The main gases whose concentrations we want to detect and measure are: H_2, CO and CH_4. the respective sensors are: MQ-8, MQ-7, MQ-4.

2.2.1 Chemical behaviour of MQ gas sensors

The basic chemical element of MQ gas sensors is a tin dioxide (SnO_2) layer. From an electrical point of view, a perfect SnO_2 crystal exhibits insulating behavior, due to its wide bandgap. Depending on the purity of the material, we note in the literature a large dispersion of the experimental values of the bandgap which varies between 2.25 to 4.3 eV [17]. On the basis of the results obtained by Jacquemin [18], we can consider that the band gap is direct and that the value of this band gap at room temperature varies between 3.5 to 4 eV. At the opposite, the real crystal has a semiconductor character. This behavior results from deviations from stoichiometry and is closely linked to the presence of oxygen vacancies leading to the presence of donor-type energy levels inside the bandgap [19].

2.2.2 Operating principle

The electrical properties of tin oxide layers are influenced by the gaseous chemical environment in contact with the layer. Thus, the absorption by physisorption or chemisorption of chemical species on the surface of the layer modifies its conductivity by a modification of the electronic states of the semiconductor by movement of electrons from the valence band towards the conduction band. This process is done in three steps [17].

Firstly, the layer is brought into contact with air and the adsorption of dioxygen molecules causes their dissociation and ionization in O- form (the most stable species at high temperature) by tearing off an electron from the band. conduction of the layer. Secondly, the reducing gas molecules, to be detected, react on the surface with the anions releasing an electron towards the conduction layer of the oxide and varying its electrical conductivity depending on the number of active oxidation sites and the number of gas molecules chemisorbed on the surface. Thirdly, following the cessation of the introduction of the gas, the oxygen present in the atmosphere adsorbs again on the surface of the oxide, returning to the equilibrium state established during the first process. However, this return to the equilibrium state assumes the absence of phenomena of poisoning of the sites by secondary molecules resulting from oxidation reactions. [19]

Given the above, the resistivity of the tin oxide layer varies depending on the concentration of environmental gases. We can model it by a variable resistance depending on the concentrations as shown on Figure 2 below.

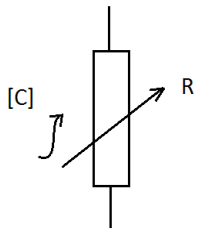

Figure 2 : Electrical model of a MQ gas sensor

2.2.3 Presentation of the sensors

The following Figure 3 is the representation of a gas MQ sensors.

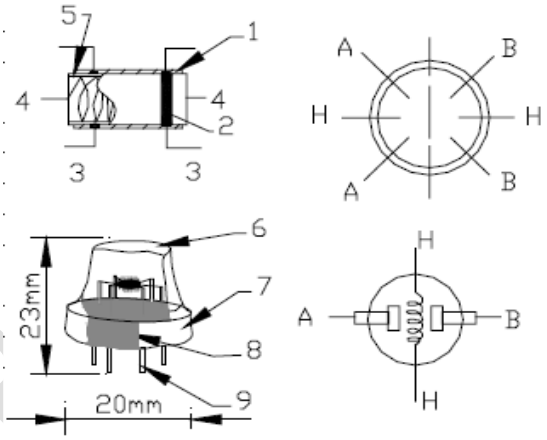

Figure 3 :MQ gas sensors structure

Each SnO_2 sensor is composed of the elements in *Table 1* below:

Table 1 : Constitutes of a gas sensor

	Parts	Materials
1	Gas sensing layer	SnO2
2	Electrode	Au
3	Electrode line	Pt
4	Heater coil	Ni-Cr alloy
5	Tubular ceramic	Al2O3
6	Anti-explosion network	Stainless steel gauze (SUS313 100-mesh
7	Clamp ring	Bakelite
8	Tube pin	Copper plating Ni

2.3 Mathematical model of the sensors

Depending on the type of sensor, the manufacturer has provided a standard catalog of correlation curves that was used.

Curves $\log\left(\frac{R_S}{R_0}\right) = f([C]_{(ppm)})$

are plotted on a logarithmic scale and are linear. By changing variables

$Y = \log\left(\frac{R_S}{R_0}\right)$ and $X = log\ ([C]_{(ppm)})$,

theses equation becomes: $Y = A * X + B$.

Using the coordinates of two points

$(X_1, Y_1)\ and\ (X_2, Y_2)$,

Wet get A and B :

$A = \frac{Y_1 - Y_2}{X_1 - X_2}$ and $B = Y_2 - \left(\frac{Y_1 - Y_2}{X_1 - X_2}\right) * X_2$

Subsequently, we will use the calibration curves provided in the technical datasheets to determine the coefficients A and B for each sensor according to the type of gas to be detected.

As said by Priyanka Kakoty and Manabendra Bhuyan: "SnO_2 based MOS gas sensors are most popular for sensing a wide range of gases. Selection of a gas sensing material is crucial due to the fact that selectivity is an important characteristic for designing efficient gas sensing devices" [20]. Therefore, the appropriate sensor for each gas will be selected in paragraphs bellow according to gas that will be sensed.

2.3.1 Dihydrogen and derivatives

These gases were detected by the MQ8 sensor.

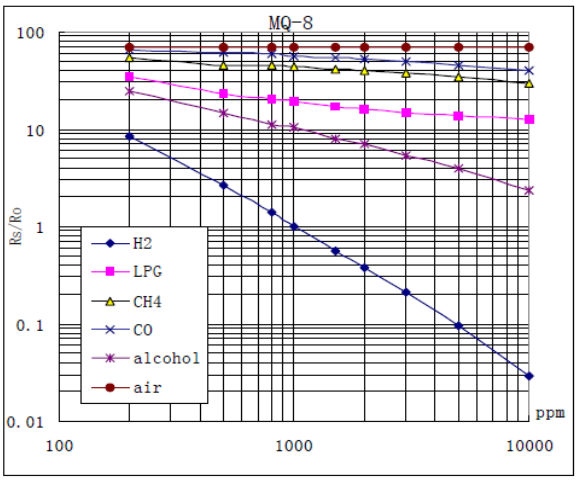

Figure 4 : MQ-8 sensitivity to different gases

As can be seen on Figure 4 above: the sensitivity of MQ-8 sensor varies depending on the gas it detects. Hydrogen has the highest variation slope, then come alcohol with a smaller slop variation. Liquefied Petroleum Gas, methane carbon monoxide has very small variation slopes, similar to that of the air. Therefore, we used MQ-8 for measuring hydrogen concentration in flue gas.

In Table 2 below, calculated the parameters A and B above for hydrogen presented.

Table 2 : Calculated values of A and B for MQ-8

AIR	70	100	0	1,845
	70	1000		
CO	Y =log (RS/R0)	X= log (ppm)	A	B
	50	3000	-0,18534	2,343
	40	10000		
CH4	Y =log (RS/R0)	X= log (ppm)	A	B
	40	2000	**-0,17875**	**2,1921**
	30	10000		
LPG	Y =log (RS/R0)		A	B
	20	800	-0,1570	1,7568
	15	5000		
ALCOL	Y =log (RS/R0)	X= log (ppm)	A	B
	4	5000	-0,61074	2,8612
	7	2000		
H2	Y =log (RS/R0)	X= log (ppm)		
	1	1000	A	B
	0,03	10000	-1,5229	4,5686

AIR
$\log\left(\frac{R_S}{R_0}\right) = 1{,}8451 \leftrightarrow \frac{R_S}{R_0} = 10^{(1{,}8451)} = 70$
H2
$\log\left(\frac{R_S}{R_0}\right) = -1{,}5228 * \log(x) + 4{,}5686$ $= A * \log(x) + B$

2.3.2 Dihydrogen carbon monoxide and others

These gases were detected with MQ-7 sensor with sensitivity characteristics reported on Figure 5 below. It can be seen there that hydrogen has the highest slop variation followed by carbon monoxide. Furthermore, the two curves were almost parallels. Therefore, in the case of gasification where carbon monoxide and hydrogen are the main components, ways should be found to determine separate concentration of either hydrogen or carbon monoxide and deduce concentration of the other.

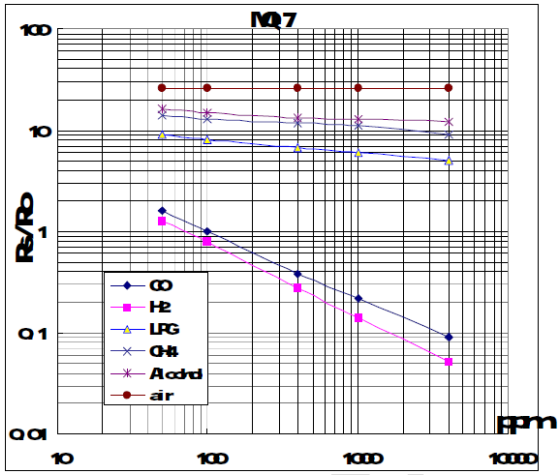

Figure 5 : MQ-7 sensitivity characteristics

Parameters A and B for MQ-7 are calculated in Table 3 : Parameters A and B calculation for MQ-7 below.

Only equation for CO is given on Table 3. H_2 was calculated from MQ-8 and deduced from MQ-7. For example, if MQ-8 reads a concentration [H_2] of hydrogen and MQ-7 reads concentration [H_2 + CO], concentration [CO] as MQ-7 reading minus MQ-8 reading was then calculated.

2.3.3 Methane and derivatives.

These gases were detected with MQ-4 sensor. Sensitivity characteristics of MQ-4 sensor is given on Figure 6 below:

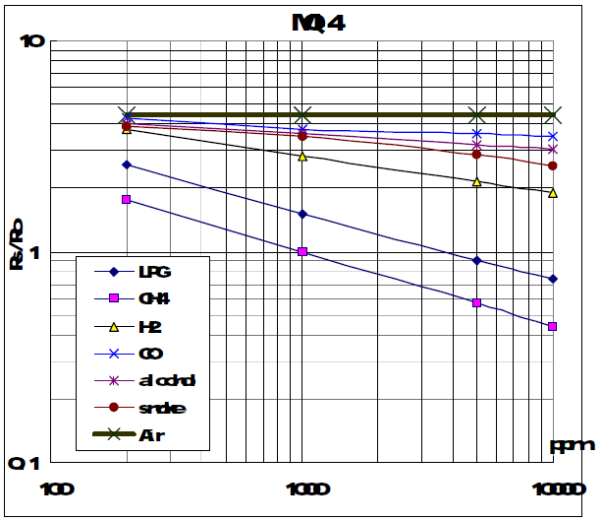

Figure 6 : Sensitivity characteristics of MQ-7

Table 3 : Parameters A and B calculation for MQ-7

Name of gas	Y =log (RS/R0)	X= log (ppm)	A	B
AIR	26	50	0	1,4150
	26	4000		
AlcohooL	Y =log (RS/R0)	X= log (ppm)	A	B
	17	50	-0,06122	1,3345
	13	4000		
CH4	Y =log (RS/R0)	X= log (ppm)	A	B
	15	50	**-0,11657**	**1,3741**
	9	4000		
LPG	Y =log (RS/R0)	X= log (ppm)	A	B
	9	50	-0,13414	1,1821
	5	4000		
CO	Y =log (RS/R0)	X= log (ppm)	A	B
	1	100	-0,65276	1,3055
	0,09	4000		
H2	Y =log (RS/R0)	X= log (ppm)	A	B
	0,8	100	-2,0588	4,0207
	0,02	600		

AIR

$$\log\left(\frac{R_S}{R_0}\right) = 1{,}415 \leftrightarrow \frac{R_S}{R_0} = 10^{(1{,}4149)} = 26$$

CO

$$\log\left(\frac{R_S}{R_0}\right) = -0{,}6527 * \log(x) + 1{,}3055$$
$$= A * \log(x) + B$$

As can see, methane has the highest variation slop on MQ-4. It is followed by LPG. We will therefore use this sensor for detecting methane in produced gases.

2.3.4 Putting these gases sensors together

In case of gasification, we seek to produce mainly carbon monoxide and hydrogen, plus sometime methane.

The stoechiometric combustion of wood in air containing 21% of oxygen and 79% of nitrogen is the following equation:

$$\boldsymbol{C_6H_{12}O_5 + 6.5(O_2 + 4.77N_2) \xrightarrow{yields} 6H_2O + 6CO_2 + 31N_2} \quad (1)$$

When oxygen is not supplied in sufficient quantity, CO is produced in lieu and place of CO_2. Also, water vapor is engaged in the so-called water-gas shift reaction that produce hydrogen as a reaction between carbon dioxide and water vapor according equation 2 to below:

$$CO + H_2O \rightleftharpoons CO_2 + H_2 \quad (2)$$

Consequently, we have mixture of CO, H_2, CH_4, CO_2 and N_2 from the gasification of biomass.

Knowing the concentrations of each of these gases thank to MQ sensors will help us monitor the gasification process.

These gases concentration will be calculated with a microcontroller as a computer under the Microchip Integrated Development Environment (IDE) named MPLAB IDE v8.80.

3. Results and discussion

3.1 Calibration of the MQ gas sensors

Calibration of MQ gases sensors mainly consist in the determination of resistance Rs. For a concentration x given in ppm, we obtain an electrical resistance Rs at the sensor output through the following properties:

3.1.1. Mathematical equations for using gas sensors

Through the calibration curves, we know that:

$$\log\left(\frac{R_S}{R_0}\right) = A * \log(x) + B$$

If we note x the gas concentration in ppm, A and B the constants depending on the type of sensor used, the we can deduce:

$$x = 10^{\left(\frac{\log\left(\frac{R_S}{R_0}\right) - B}{A}\right)} \text{ or also}$$

$$\frac{R_S}{R_0} = 10^B * x^A \text{ or also}$$

$$x = \left(\frac{R_S}{R_0} * 10^{-B}\right)^{\frac{1}{A}}$$

We have summarized the values obtained for A and B in the two Table 4 and Table 5 below.

Table 4 :Parameter A values of the 3 gas sensors

MQ4 (CH4)	MQ7 (CO)	MQ8 (H2)
$-\mathbf{0},3072$	$-0,6527$	$-1,522$

Table 5 : Parameter B values of the 3 gas sensors

MQ4 (CH4)	MQ7 (CO)	MQ8 (H2)
0,921	1,3055	4,5686

Hence the following mathematical functional block in steady state for each sensor:

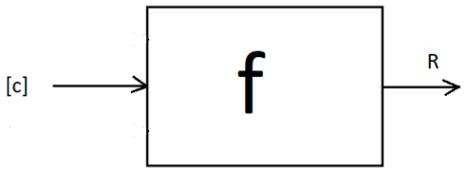

Figure 7 : Functional bloc of the sensors

[C]=x: concentration of the inlet gas.
R=Rs: output resistance.

f: the mathematical steady-state input-output correlation function.

3.1.2. Measurement range

The Table 6, Table 7 and Table 8 above represent the measurement ranges of the sensors.

Table 6 : H2 : MQ8

X= [C] (ppm)	100	10000
RS (kΩ)	10	60

Table 7 : CO : MQ-7

X= [C] (ppm)	10	10000
RS (kΩ)	2	20

Table 8 : CH4 : MQ-4

X= [C] (ppm)	100	10000
RS (kΩ)	10	60

3.1.3 Intrinsic sensitivity of the sensors

The intrinsic sensitivity of sensors for a variation ΔR of the output, can be estimated through the input variation Δx.
It is equal to:

$$\frac{\partial x}{\partial R_s} = \frac{1}{A} * \left(\frac{10^{-B}}{R_0}\right) * \left(\frac{R_s}{R_0} * 10^{-B}\right)^{\left(\frac{1-A}{A}\right)}$$

3.1.4 Implementation in MPLAB IDE

MPLAB IDE is written in C language. Equation from different sensors were derived for each sensor and we obtained results summarized below.

Figure 8 : Microchip MPLAB IDE logo

```
void main(void)   // main fonction
{

init_uc(); //microcontroleur initialisation


 while(1)   // loop
 {

  // mesurment of gas contration
    if(gaz_process==1)
     {
        gaz_process=0;
        acquisition ();
       integration(0);
      gaz_processing (0);
      integration(1);
      gaz_processing (1);
     }

      // measurement of humidity
      if(fin_hum)
      {
        fin_hum=0;
         humidity_processing ();
      }
```

Figure 9 : The main bloc of our program

As we can see on Figure 9 above, the main program is subdivided in six routines that do

a given work. The most important of these is “gaz_processing ( )” that calculate the different concentrations of the gases as illustrated on Figure 10 below:

```
void gaz_processing (int8 canal_in)
// gas concentrartion measurement fonction
{
  float yy, xx,m, b0;
  int16 reste;
// computing of correction coefficients
// according to humidity
k_rh_mq4= (val_humidity /-322.6)+ 1.10;
k_rh_mq7= (val_humidity/-370.4)+ 1.09;
     if(canal_in==0)
     {
      k_r=1.1560;  //k_r= rl_mq7/r0_mq7;
      //k_g=0.889024;

      k_t_mq7=0.9408;  //à 34 degré celcius
      k_g= k_t_mq7  * k_rh_mq7;
      m=1.0/a_mq7;
      b0=20.2069143  ;//b0= pow(10,b_mq7);
       vs=vs_mq7;
     }

     if(canal_in==1)
     {
      k_r=1.1599;  //k_r= rl_mq4/r0_mq4;
      //k_g=0.887494;

       k_t_mq4=0.9578;
       k_g= k_t_mq4  * k_rh_mq4;
       m=-3.25520833;//m=1.0/a_mq4;
       b0=8.33681185  ;//b0= pow(10,b_mq7);
       vs=vs_mq4;
     }
```

Figure 10 : The gases concentrations calculation function of the program

3.2 Electronic prototype

From the electronic diagrams, we were able to create some prototype power supply and conditioning boards (and). The measurement cards are made with Pic-kit cards from Microchip and Arduino uno. The measurement system was fabricated with prototyping board and assembled together. The power supply board provides 5V, +8V and -8V voltages to the sensors and measurement amplifiers as seen below:

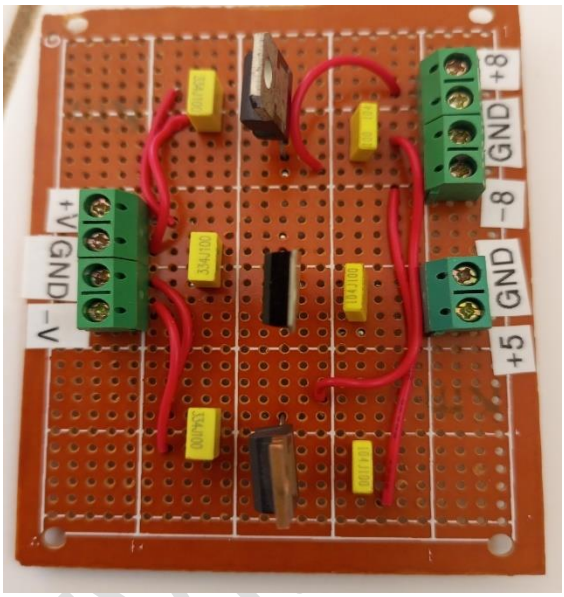

Figure 11 : Main power module

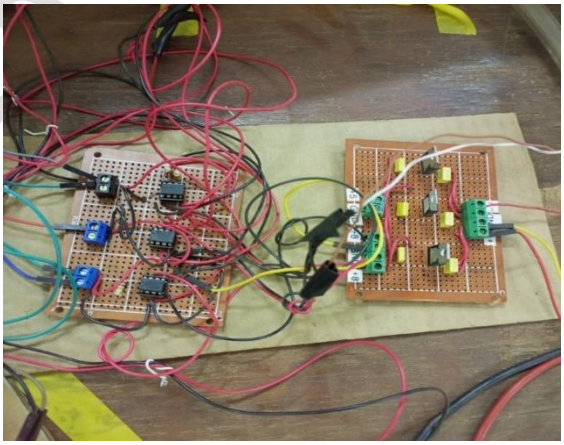

Figure 12 : Treatment and power supply boards

3.4 Tests results

On September 23, 2023, gasification measurement tests were carried out and obtained CH4 concentration values = 310 ppm; CH4=10ppm; RH= 72%. Figure 13 represents a local display on an LCD screen of the gasification parameters obtained during the test.

These values were lesser than those we go from previous experiments in nearly similar

experimental conditions: waste weigh, weather, etc.

Figure 13 : Test results on LCD display

These measurement results show low production of combustible gas. The air-dried wood used did not seem to have any problems and it had not rained in the 2 days preceding our handling. At that time, the oxygen concentration measurement module was not yet ready and we did not understand the reason for the failure of our manipulation. On November 1, 2023 at 5 p.m., we then took measurements of the humidity level of the ambient air. There we found 51%. On January 10, 2024, the indicated humidity level was 8%. We then looked for the causes of these differences in values and consulted the history of the weather in Koudougou. So, for September 23, 2023, the following screenshot shows that the weather forecast indicated between 65 and 75% air humidity:

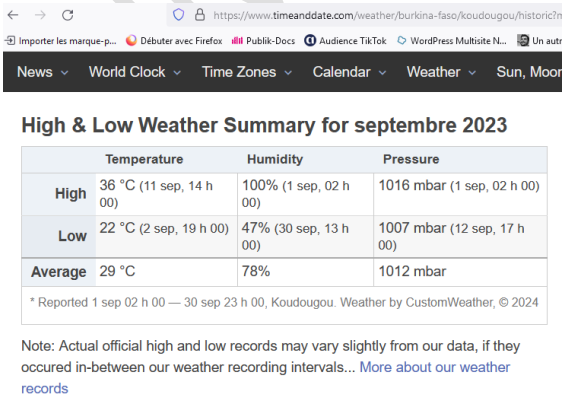

Figure 14 : Weather in Koudougou during September 2023

Conclusion therefore made that our gas measurement system is working as intended.

4. Conclusion

Through this study, the operation of gas concentration sensors made by Hanwey Corp was highlighted. The test body of these sensors is a layer of tin dioxide (SnO_2) whose resistivity is sensitive to contact gases and varies according to their concentration. The electrical model of these sensors is a resistance R whose measurand is the concentration x of the gas in contact of the sensor. There is a relation of the form: $\log (R/R_0) = A \log (x) + B$, with A= -0.3072, B = 0.921 for methane, A= -0.6527, B=1.3055 for carbon dioxide and A= -1.522, B = 4.5686 for hydrogen. CO concentration of 310 ppm and CH_4 concentration of 10ppm was measured. The same method was applicable for H_2. However, these sensors were are sensitive to the temperature and humidity of the gases measured. These auxiliary parameters will be investigated in order to find the real physical and mathematical model allowing judicious exploitation of these sensors. Also, except for hydrogen with MQ-8, sensor selectivity is not very good. In case of gasification, MQ7 would indifferently measure hydrogen and carbon monoxide concentration.

5. REFERENCES

1 Joan Nyika, Adeolu Adesoji Adediran, Adeniyi Olayanju, Olanrewaju Seun Adesina and Francis Odikpo Edoziuno, The Potential of Biomass in Africa and the Debate on its Carbon Neutrality, Biotechnological Applications of Biomass, DOI: 10.5772/intechopen.93615, 2020

2 Sustainable Energy for All, [Burkina Faso]: Rapid assessment and gap analysis, pp. 1-2, https://www.seforall.org/sites/default/files/Burkina_Faso_RAGA_FR_Released.pdf, Accessed 26 septembre 2023. French.

3 Nzihou Jean Fidele, Hamidou Salou, Imbga Kossi, Segda Bila Gerard, Ouattara Frederic, Tiemtore Hamadou, Electrical Power Generation from Heat Recovered at the throat of a Downdraft Biomass Gasifier, American Journal of Science, Engineering and Technology, 2023; 8(3) : 133-140, http://www.sciencepublishinggroup.com/j/ajset ISSN: 2578-8345 (Print); ISSN: 2578-8353 (Online)
doi: 10.11648/j.ajset.20230803.12, 2023

4 Nzihou Jean Fidele, Hamidou Salou, Segda Bila Gerard, Ouattara Frederic and Compaore Hamidou, Effects of a Cyclone Dimensions on Quality of Syngas Produced with a Wood-fired Biomass Gasifier, Journal of Energy Research and Reviews, Article number JENRR.107030, ISSN: 2581-8368, Volume 15, Issue 3, Page 1-14, 2023

5 Reed TB, Das A, Handbook of Biomass Downdraft Gasifier Engine Systems, Solar Energy Research Institute; 1950.
Available:
https://www.nrel.gov/docs/legosti/old/3022.pdf, accessed 15 September 2023

6 Akhator P. E., Obanor A. I. and Sadjere E. G., Design and development of a small-scale biomass downdraft gasifier, Nigerian Journal of Technology (NIJOTECH) Vol. 38, No. 4, October 2019, pp. 922 – 930 Print ISSN: 0331-8443, Electronic ISSN: 2467-8821 http://dx.doi.org/10.4314/njt.v38i4.15

7 Mukunda H. S., Dasappa S., Paul P. J., Rajan N. K. S., and Shrinivasa U., "Gasifiers and combustors for biomass - technology and field studies," Energy for Sustainable Development, vol. 1, no. 3, pp. 27-38, 1994.

8 Abubakar A. Bukar, M. Ben Oumarou, Babagana M. Tela, Abubakar M. Eljummah Assessment of Biomass Gasification: A Review of Basic Design Considerations, American Journal of Energy Research, Vol. 7, No. 1, 1-14. 2019.

9 Chawdhurya M. A. and Mahkamovb K.. Development of a Small Downdraft Biomass Gasifier for Developing Countries. JOURNAL OF SCIENTIFIC RESEARCH J. Sci. Res. 3 (1), 51-64 (2011) www.banglajol.info/index.php/JSR

10 Yulin Kong, Yuxiu Li, Xiuxiu Cui, Linfeng Su, Dian Ma, Tingrun Lai, Lijia Yao, Xuechun Xiao, Yude Wang, SnO_2 nanostructured materials used as gas sensors for the detection of hazardous and flammable gases: A review, Nano Materials Science, Volume 4, Issue 4, 2022, Pages 339-350, ISSN 2589-9651, https://doi.org/10.1016/j.nanoms.2021.05.006. 2022

11 Kadek I NuaryTrisnawan, Agung Nugroho Jati, Novera Istiqomah, Isro Wasisto, Detection of Gas Leaks Using The MQ-2 Gas Sensor on the Autonomous Mobile Sensor,

12 Nisal Kobbekaduwa, Pahan Oruthota and W.R. de Mel, Calibration and Implementation of Heat Cycle Requirement of MQ-7 Semiconductor Sensor for

Detection of Carbon Monoxide Concentrations, Advances in Technology. 2021, 1(2), 377-392

13 Sohibun, I Daruwati, R G Hatika and D Mardiansyah, MQ-2 Gas Sensor using Micro Controller Arduino Uno for LPG Leakage with Short Message Service as a Media Information, URICSE 2021, Journal of Physics: Conference Series, (2021) 012068 IOP Publishing, doi:10.1088/1742-6596/2049/1/012068

8 Abubakar Yakub Nasir1, U. I. Bature2, N. M. Tahir3, A. Y. Babawuro4, Adoyi Boniface5 A. M. Hassan, Arduino based gas leakage control and temperature monitoring system, International Journal of Informatics and Communication Technology (IJ-ICT), Vol.9, No.3, December 2020, pp. 171-178, ISSN : 2252-8776, DOI : 10.11591/ijict.v9i3.pp171-178 Journal homepage: http://ijict.iaescore.com, 2020

15 Huan Hui Yan, Yusnita Rahayu, Design and Development of Gas Leakage Monitoring System using Arduino and ZigBee, Proceeding of International Conference on Electrical Engineering, Computer Science and Informatics (EECSI 2014), Yogyakarta, Indonesia, 20-21 August 2014

16 Dewi L and Somantri Y, Wireless sensor network on lpg gas leak detection and automatic gas regulator system using Arduino, IOP Conf. Serie: Material Sciences Engineering, 384 012064, 2018

17 Laghrib Souad, Synthesis of Thin Films of: SnO2, SnO_2: In by Two Physical and Chemical Processes and Study of Their Characterization, PhD Thesis, Ferhat Abbas University, Algeria, 139 pages, 2018. French.

18 Jacquemin J. Optical PROPERTIES OF Intrinsic SnO2 AND β-PbO_2 neighborhood of the gap. Journal de Physique Colloques, 1974, 35 (C3), pp. C3-255-C3-260. 10.1051/jphyscol:1974337. jpa-00215585

19 Laghrib Souad, Hania Amardjia-Adnani, Dahir Abdi, Jean-Marc Pelletier, Development and study of thin layers of SnO_2 obtained by evaporation under vacuum and annealed under oxygen, Revue des Energies Renouvelables Volume 10 N°3 (2007) 357–366, 2007. French.

20 Priyanka Kakoty and Manabendra Bhuyan, $Sn0_2$ based gas sensors: Why it is so popular?